

RESEARCH

Open Access



Prediction of Chloride Penetration Depth Rate and Diffusion Coefficient Rate of Concrete from Curing Condition Variations due to Climate Change Effect

Tae-Kyun Kim, Seung-Jai Choi, Ji-Hun Choi and Jang-Ho Jay Kim*

Abstract

Recently, many countries including Korea are experiencing serious climatic events, such as heat waves, torrential rain, cold waves, heavy snowfall, and typhoons. In addition, due to the extreme climate events, the construction period of concrete structures tends to be extended, whereby increasing related economic losses. Pushing through construction projects without considering climate change results in low-quality concrete, causing poor constructions humans and consequent casualties and property damages. Moreover, exposure of concrete structures to extreme environmental conditions that involve carbonation, freezing and thawing and to chloride attack environments may reduce the durability of concrete. In the environments of carbonation and chloride attack, concrete structure cured in inadequate curing conditions develops cracks, making it easy for CO₂ and chloride to and corrode rebars and reducing durability of concrete. Also, in the environments of repeated freezing and thawing, the inadequately cured concrete develops microcracks through which water infiltrates, resulting in decline in performance. According to the study results, durability generally declines most rapidly in the chloride attack environment among various environmental types. Therefore, to address these issues and provide measures for climate change, this study investigated the effect of climate factors on strength and chloride diffusion coefficient rate of concrete structure by selecting sunlight exposure time and wind speed as the most important curing conditions among various climate factors that affect concrete performance. Regarding the analytical method of experimental results, performance based evaluation (PBE) on concrete strength and durability using Satisfaction Curve is proposed. In addition, the PBEs used in this study are applied to future climate scenarios. It is expected that the optimal mix ratio accounting for climatic change in concrete mixing can be derived using the future climate change scenario.

Keywords: climate change, chloride diffusion coefficient rate, Satisfaction Curve (SC), performance based evaluation (PBE)

1 Introduction

Recently, extreme climate change has been occurring globally. In addition to changes in average temperature and precipitation, climate change manifests as an increase in the frequency of draught, floods, and heat waves, and growing strengths of tropical cyclones such as hurricanes

and typhoons, as a result of changes in precipitation and temperature. In general, when air temperature increases by 1 °C, the water content in the atmosphere increases by approximately 7%, increasing the frequency of heavy rainfall and draught (Kwon 2005). Korea's weather phenomena are not an exception. According to the Korea Meteorological Administration (KMA), the average temperature of the six major cities in Korea increased by approximately 1.5 °C since 1900, which is almost twice as the average increase in global temperature (Weather Knowledgebase 2012). Moreover, compared to the 1920s,

*Correspondence: jjhkim@yonsei.ac.kr
School of Civil and Environmental Engineering, Yonsei University, 134
Shinchon-dong, Seodaemun-gu, Seoul 03722, South Korea
Journal information: ISSN 1976-0485 / eISSN 2234-1315

the length of winter has decreased by approximately 30 days, while the length of spring and summer was approximately 20 day longer, suggesting the continuing temperature increase is changing the length of seasons. Despite large variation across decades, annual average precipitation also shows the increasing trend, and the intensity of rainfall shows the increasing trend, as the number of days with precipitation decreases and the precipitation increases in general (KMA 2008). In addition, climate change can manifest as climate extremes such as heat waves, torrential rain, and heavy snowfall (Myong 2009). Due to the extreme climate events, the construction period of concrete structures at construction sites tends to be extended, increasing related economic losses. Pushing through construction projects without considering climate change results in low-quality concrete, leading to weak constructions. Concrete is exposed to various climatic factors during the curing process. Concrete is exposed to various climate environments in the curing process. In particular, concrete structures require appropriate early hydration to have proper strength development. However, when relative humidity decreases or temperature increases rapidly outside, cracks due to high temperature or long-term strength degradation occur due to water evaporation inside concrete. On the other hand, when temperature is low, strength degradation occurs as setting and curing are delayed significantly. In addition, constant exposure to wind and sunlight during curing causes water movement and evaporation as well as temperature fluctuations in specimens, which produce cracks and various problems with material properties as a result of sharp increases in hydration temperature. These suggest that various curing conditions caused by climate change are likely to result in concrete strength degradation by causing porosity and microcracks inside concrete (Kato et al. 2005; Thomas and Bamforth 1999; Mangat and Gurusamy 1987).

In particular, exposure of concrete structure to extreme environmental conditions such as carbonation, freezing and thawing, and chloride attack environments may reduce durability of concrete (Poon et al. 2006; Luping and Nilsson 1992; Leng et al. 2000). In the environments of carbonation and chloride attack, concrete structure that cured in inadequate curing conditions develops cracks, making it easy for CO₂ and chloride to penetrate and corrode rebars, and reducing durability of concrete (Park and Choi 2012; Morga and Marano 2015; Ramseyer and Kang 2012; Divsholi et al. 2014; Elsafty and Abdel-Mohti 2013). Also, in the environments of repeated freezing and thawing, the inadequately cured concrete develops microcracks through which water infiltrates, resulting in decline in performance (Jang et al. 2011; Oh and Jang 2003; Dhir and Jones 1999). According to the

study results, durability generally declines most rapidly in the chloride attack environment among various environmental types (Arribas et al. 2014; Chen et al. 2014; Alqam and Alkam 2014; Ye et al. 2015).

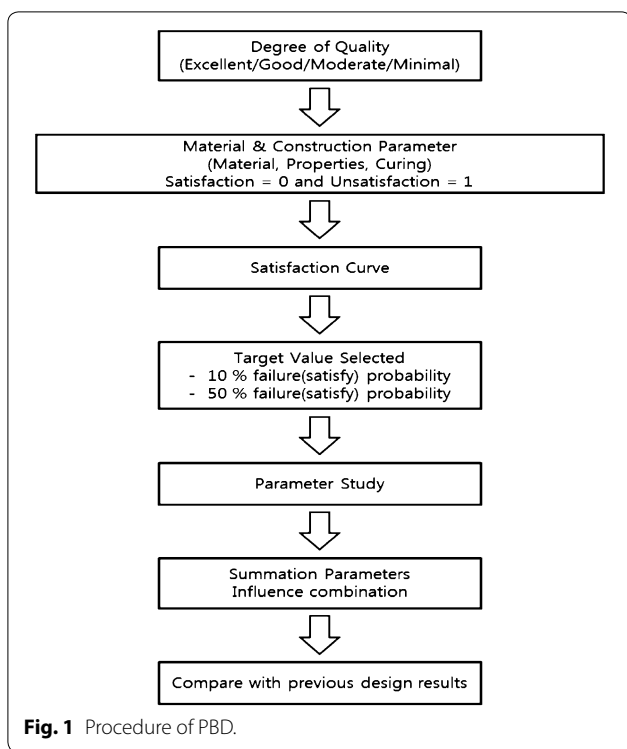
Therefore, to address the problems caused by climate change and provide suitable responses, this study involved a chloride diffusion coefficient rate experiment in which concrete, of the various climatic factors that affect concrete curing, was cured under variable wind speed and sunlight exposure conditions and exposed to extreme environments. Regarding the analytical method of experimental results, performance based evaluation (PBE) of concrete strength and durability using Satisfaction Curve is proposed.

2 Procedure of Performance Based Evaluation (PBE)

2.1 Performance Based Evaluation Theory

The performance based evaluation (PBE) to be used in this study is an evaluation method based on performance based mixture design (PBMD) in a previous study. The procedure of PBMD is as follows. The design process of PBMD is the process of finding the optimal concrete mixing using the concept of the SC, and largely consists of three stages. The first stage is the initial design process based on the client's request. The second stage is the process of evaluating and optimizing the initial design and the third stage is revising the intermediate design and completing a final design. To be more specific, the first stage is divided into Steps 1 and 2, and the second stage into Steps 3 and 4, and the third stage into Steps 5, 6, and 7.

As shown in Fig. 1, in Step 1, the designer must understand the client's request accurately. In Step 2, based on client's requirements, material properties, target design standards, and structure performance rating are determined, and initial standard mix is prepared. In Step 3, performance of the initial design is evaluated by collecting data and plotting SCs, and in Step 4, multiple SCs are combined into a single SC, using the influence coefficient rate and the concept of effective influence value. In Step 5, the actual performance and the performance standard initially established are compared, and based on the results of the comparison, in Step 6, concrete proportioning is modified followed by optimization of proportioning. Finally, in Step 7, it is verified whether final concrete proportioning meets the client's requirements (Kim et al. 2011). However, as this study is an evaluation of concrete safety and durability, the procedures up to Step 3, evaluating the design by plotting SCs, were performed. In addition, previous studies examined performance based mixture design (PBMD) related to concrete mixing only, whereas this study conducted a performance based evaluation (PBE) from a climate



perspective for the first time (Kim et al. 2011, 2012; Phan et al. 2012).

3 Experimental Method

3.1 Concrete Mixture and Curing Conditions

Table 1 shows details of the concrete mixture, with coarse aggregate of 25 mm, w/c of 55%, and design strength of 27 MPa. Table 2 shows concrete curing conditions regarding sunlight exposure time and wind speed. The conditions were decided based on the examination of the last 10 year data from Korea Meteorological Administration (KMA) for Seoul, Korea, and the specifics of the conditions were decided based on the precedents in previous studies (Kim et al. 2014, 2015).

3.2 Concrete Chloride Diffusion Coefficient Rate Theory

In the case of reinforced concrete structure, performance deterioration occurs during curing conditions by chemical and physical causes in various environments. One of the prime examples of concrete performance degradation

Table 2 Concrete curing conditions (Kim et al. 2015).

Case	Wind speed (m/s)	Sunlight exposure time (h)	Case	Wind speed (m/s)	Sunlight exposure time (h)
1	0	2	9	4	2
2	0	4	10	4	4
3	0	6	11	4	6
4	0	8	12	4	8
5	2	2	13	6	2
6	2	4	14	6	4
7	2	6	15	6	6
8	2	8	16	6	8

is the decrease in durability of concrete structure in chloride attack environment. When chloride permeates into concrete and attaches to reinforcing bars due to chloride attack environment and the use of deicing salt in winter, it causes corrosion of reinforcing bars, which leads to reduced cross-sectional area and falling off concrete. Thence, the concrete structure does not perform properly.

Regarding estimation methods of concrete chloride diffusion coefficient rate, Fick’s First Law can be used in a steady state, and Fick’s Second Law is used in a non-steady state. As the present study conducted an experiment where chloride diffusion was promoted, it can be considered as a non-steady state.

In addition, experiments on concrete chloride diffusion in domestic and international studies are mainly conducted using four methods, as shown in Table 3. ASTM C 1202 can measure the amount of the passing charge using diffusion cell, and the total amount of time required is 6 h. NT Build 355 can measure concentration increase, and the total amount of time required is 1–2 months. NT Build 443 can measure salinity penetration profile, and the minimum amount of time required is 1 month. Finally, NT Build 492 can measure chloride penetration depth rate and the diffusion coefficient rate based on the depth rate, and it takes 24–48 h to complete.

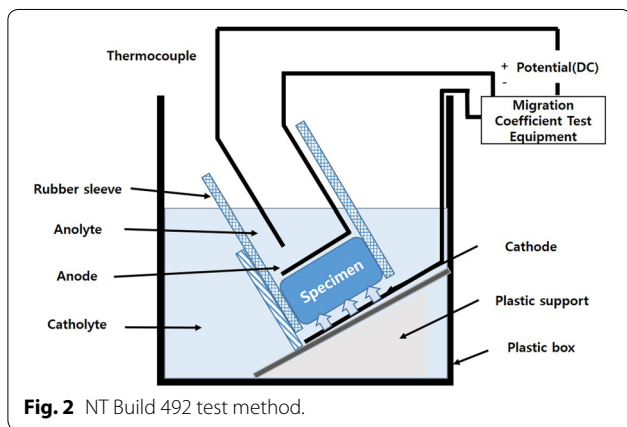
This study focuses on measuring diffusion coefficient rate of chloride ion, and accordingly employed NT Build 492, studied by researchers such as Nilsson and Tang in Europe (Tang and Nilsson 1992).

Table 1 Mix proportion of concrete (Kim et al. 2015).

Coarse aggregate size (mm)	w/c (%)	Unit (kg/m ³)				f _{ck} (MPa)
		Water W	Cement C	Fine aggregate S	Coarse aggregate G	
25	55	183	333	677	1014	27

Table 3 Concrete chloride experimental type.

Code	Name	Volt
ASTM C 1202	Standard test method for electrical indication of concrete ability to resist chloride ion penetration	60 V
NT Build 492	Chloride migration coefficient from non-steady state migration experiments	10–60 V
NT Build 355	Chloride diffusion coefficient from migration cell experiments	12 V
NT Build 443	Accelerated chloride penetration	–



3.3 Experimental Method of Concrete Chloride Diffusion Coefficient Rate

Wind speed and sunlight exposure time curing shown in Table 2 was conducted for 28 days, and the experiment based on NT Build 492 was conducted after curing. Experimental method is as follows. Circular specimen of $\varnothing 100 \times 200$ mm is cut in thickness of 50 ± 2 mm. The cut specimen is placed in a vacuum desiccator and kept in a vacuum state with absolute pressure of 10–50 mbar (1–5 kPa) for 3 h. The CaOH_2 solution is then added for the specimen to be immersed, and kept in a vacuum state for 18 ± 2 °C to saturate the specimen. As shown in Fig. 2, for the saturated specimen, the positive electrode is filled with 0.3 N NaOH solution (approximately 12 g NaOH in 1 l water) and the negative electrode is filled with 10% NaCl solution (100 g NaCl in 900 g water, about 2 N). The initial voltage of 30 V is applied, and additional voltage to be applied is determined by measuring initial current. Finally, depending on the amount of the current, measurement is conducted for 6 h at minimum and 96 h at maximum.

After completing the experiment, the specimen is taken out and cut in half, which is followed by spraying the solution mixed with AgNO_3 onto the specimen, and measuring the part where color of specimen changes. The measurement method is as follows. As shown in Fig. 3, seven sites, except the 10 mm at both ends of the specimen, are measured in a constant interval, and their

mean is obtained. Both ends are excluded from measurement because they can be contaminated by the solution that penetrates during the experiment.

4 Test Results

4.1 Concrete Strength

Table 4 and Fig. 4 show the results on concrete strength in various wind speed and sunlight exposure time conditions (Kim et al. 2015). When the concrete specimens cured under different wind speed and sunlight exposure time conditions are compared with specimens cured with dry air, the specimens cured under 0 m/s wind speed and all sunlight exposure time conditions showed similar strength trends. However, with respect to other wind speed and sunlight exposure time conditions used in the study, the specimens showed the largest 3-day and 7-day strengths when cured in a wind speed of 2 m/s sunlight exposure time of 8 h conditions. These results likely occurred due to stronger sunlight exposure increasing the concrete surface and internal temperatures. Therefore, it can be concluded that the higher early curing temperature produces, the higher early strength due to the faster hydration reaction. However, in conditions with wind speed higher than 0 m/s, the specimens showed normal early strength development of 3-day and 7-day strengths, by showing at least 40% and 70% of the 28-day compressive strength of 27 MPa. In contrast, the 28-day long-term strength was approximately 45% lower than the design strength of 27 MPa, and the similar trend was found in splitting tensile strengths. Meanwhile, the specimens cured under wind speed of 2 m/s, 4 m/s, and 6 m/s conditions with varying sunlight exposure time, 28-day compressive strengths were slightly greater for specimens cured at 6 m/s than at 2 m/s and 4 m/s, regardless of the sunlight exposure time. In this study, three specimens cured under the same condition are tested and the average strength is used for comparison. A minimal of three specimen test results would give the minimal errors. Thereby reducing the errors and increasing results accuracy. However, if more number of specimen test results is available, the accuracy can be increased. For the purpose of mixing verification, the results on strengths of specimens from water curing and thermo-hydrostatic curing were also obtained, and they showed strengths of 38.32 MPa and 31.11 MPa, respectively, which were above

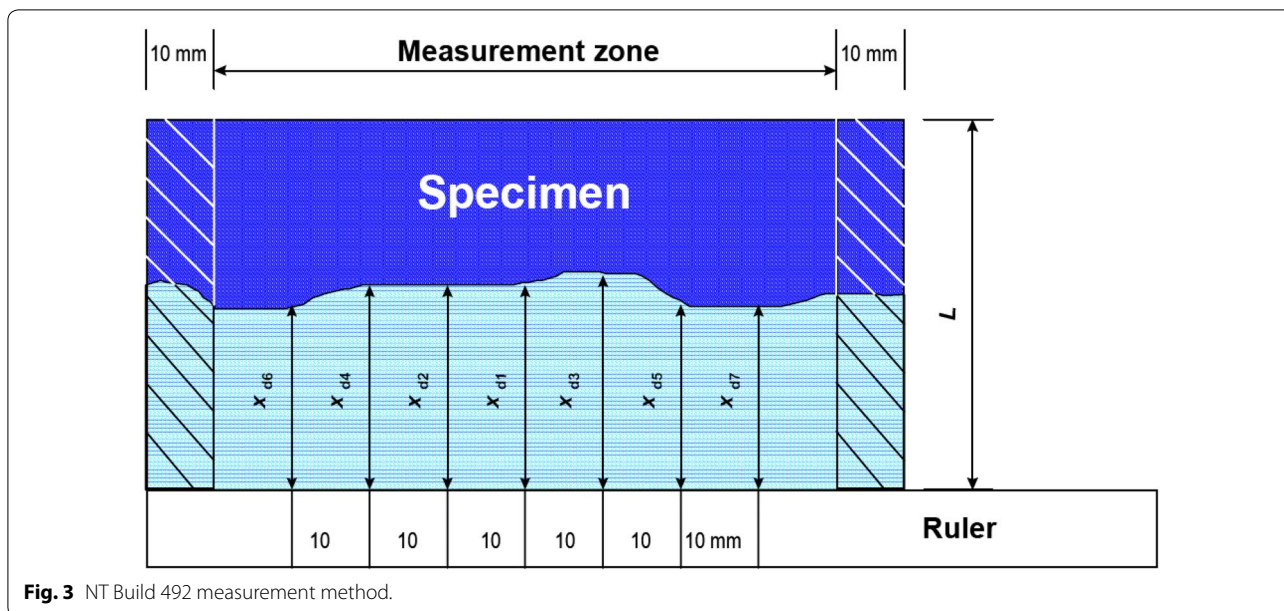


Fig. 3 NT Build 492 measurement method.

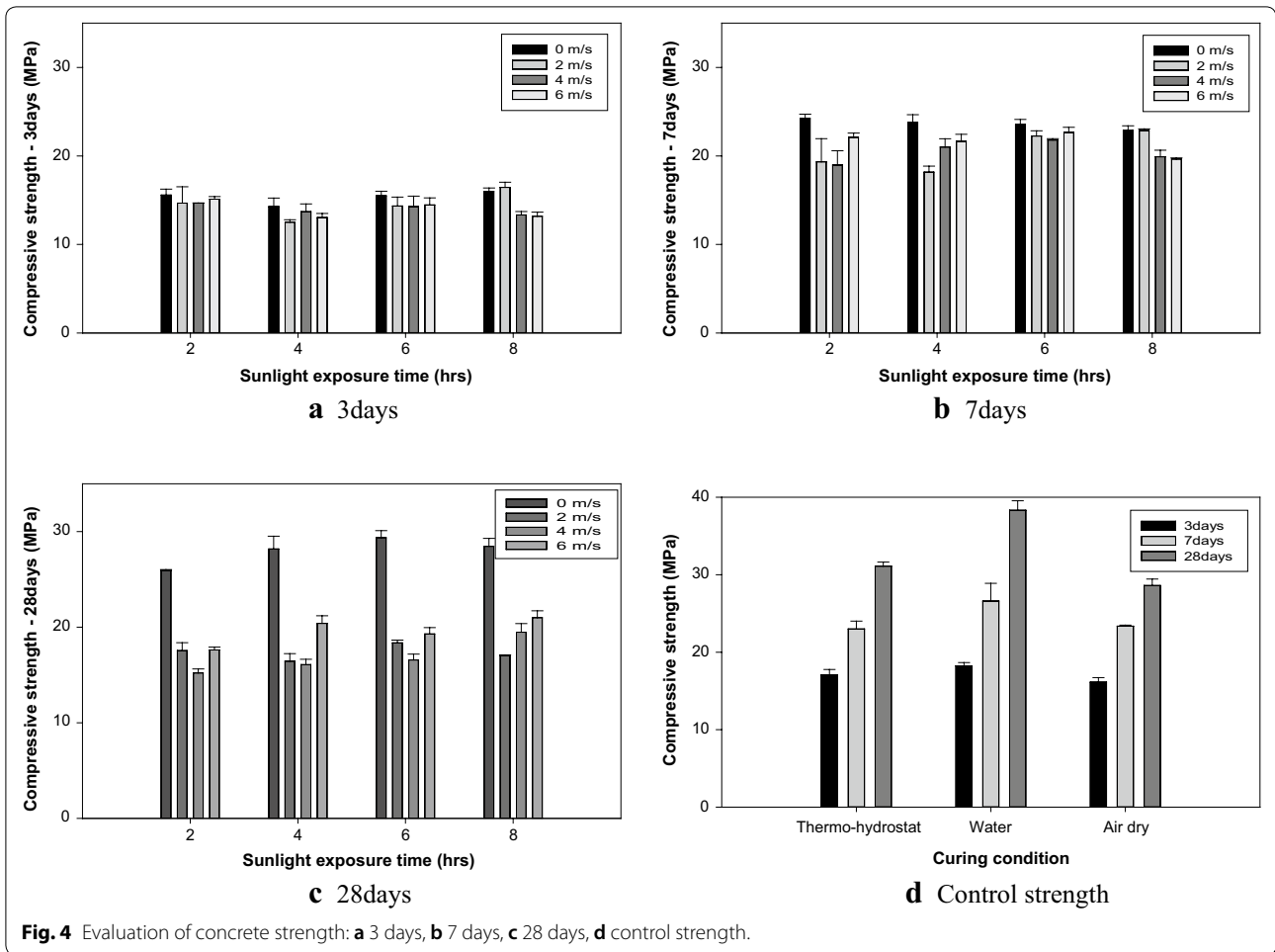
Table 4 Strength test results of wind speed–sunlight exposure time (Kim et al. 2015).

Case	Wind speed (m/s)	Sunlight exposure time (h)	Compressive strength (MPa)			Splitting tensile strength (MPa)		
			3 days	7 days	28 days	3 days	7 days	28 days
1	0	2	15.57	24.24	25.94	1.45	1.92	2.12
2	0	4	14.28	23.78	28.18	1.4	1.9	2.22
3	0	6	15.49	23.55	29.36	1.39	1.9	2.4
4	0	8	15.99	22.87	28.46	1.52	1.95	2.05
5	2	2	14.66	19.34	17.55	1.3	2.2	2.07
6	2	4	12.51	18.17	16.44	1.6	1.94	1.65
7	2	6	14.34	22.25	18.36	1.48	2.05	2.02
8	2	8	16.45	22.87	17	1.59	2.17	1.93
9	4	2	14.66	18.97	15.21	1.6	1.98	2.17
10	4	4	13.7	21.01	16.08	1.68	1.99	2.02
11	4	6	14.27	21.8	16.57	1.7	2.14	1.83
12	4	8	13.33	19.91	19.48	1.46	2.21	1.71
13	6	2	15.11	22.1	17.62	1.74	2.16	1.95
14	6	4	13.03	21.65	20.4	1.6	2.18	1.78
15	6	6	14.46	22.66	19.29	1.61	2.05	2
16	6	8	13.18	19.65	21	1.33	2.23	1.7
Control specimens								
Thermo-hydrostatic curing	0	0	17.06	23	31.11	1.58	2.18	2.25
Wet curing	0	0	18.24	26.6	38.32	1.72	2.29	2.7
Air dry curing	0	0	16.13	23.36	28.61	1.36	1.84	2.2

the design strength. These results suggest that wind speed and sunlight exposure curing conditions resulted in lower concrete strengths because of inadequate hydration caused by water movement from sustained wind, and water evaporation from sunlight exposure.

4.2 Chloride Depth Rate and Chloride Diffusion Coefficient Rate

Tables 5 and 6 and Figs. 5 and 6 show the results on chloride diffusion coefficient rate. The coefficient rate is obtained by measuring chloride penetration depth rate and



defined by Eqs. (1)–(3) based on the depth rate (NT Build 492, 1999).

$$D_{nssm} = \frac{RT}{zFE} \times \frac{X_d - \alpha \sqrt{X_d}}{t} \tag{1}$$

where

$$E = \frac{U - 2}{L} \tag{2}$$

$$\alpha = 2\sqrt{\frac{RT}{zFE}} \cdot \text{erf}^{-1}\left(1 - \frac{2c_d}{c_0}\right) \tag{3}$$

D_{nssm} denotes the potential difference promoting chloride ion diffusion coefficient rate (m^2/s), R denotes the gas constant ($8.314 \text{ J/(K}\cdot\text{mol)}$), T denotes the absolute temperature (K), L denotes the thickness of specimen (m), z denotes ion electron value ($z=1$ for chloride), F denotes the Faraday constant ($9.648 \times 10^4 \text{ J/(V}\cdot\text{mol)}$),

Table 5 Test results of concrete chloride depth rate (mm).

Wind speed	Sunlight exposure time			
	2	4	6	8
0	30.81	31.44	35.79	37.18
2	37.46	37.88	37.92	39.21
4	38.75	43.31	43.47	47.31
6	44.48	47.12	45.76	47.57

Thermo-hydrostatic curing: 25.27 (chloride depth rate of chamber-cured concrete at 20°C temperature and ± 95% relative humidity)

Wet curing: 22.11 (chloride depth rate of water-cured concrete at 20 °C temperature and 100% relative humidity)

Air dry curing: 29.77 (chloride depth rate of air-cured concrete at 20 °C temperature and ± 60% relative humidity)

U denotes the potential difference (V), X_d denotes the mean depth rate of penetration based on the colorimetric method (m), t denotes the time applied for the potential difference (s), C_0 denotes chloride ion concentration of cathode cell ($\approx 2 \text{ N}$), C_d denotes reaction concentration

Table 6 Test results of concrete chloride diffusion coefficient rate ($\times 10^{-12} \text{ m}^2/\text{s}$).

Wind speed	Sunlight exposure time			
	2	4	6	8
0	46.11	47.16	54.5	57.44
2	57.54	58.24	58.3	61.19
4	58.38	65.7	66	73.29
6	69.94	74.25	71.85	75.89

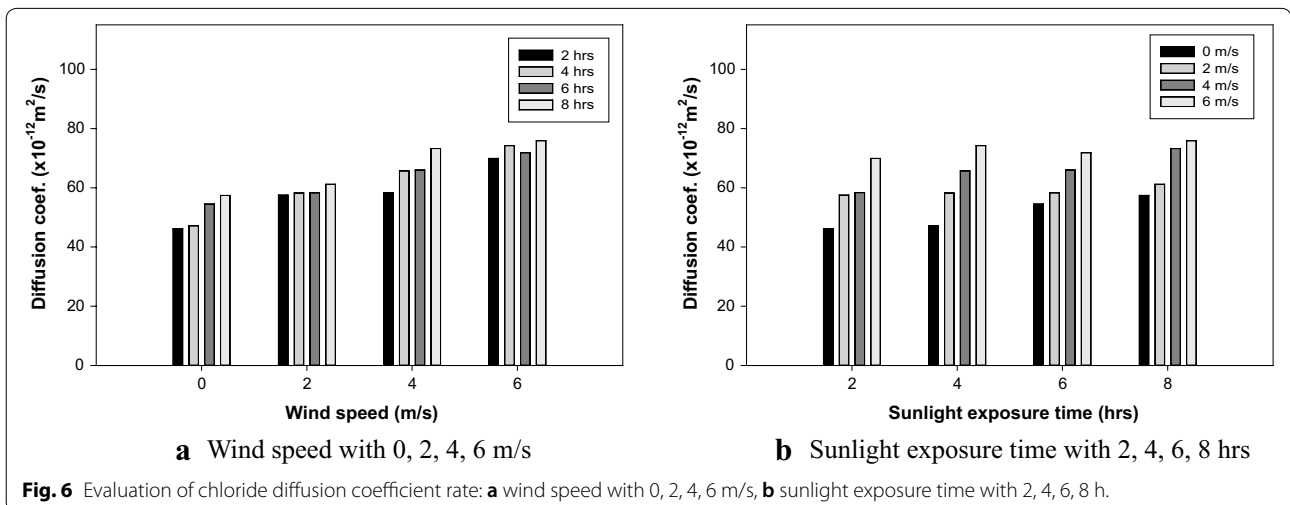
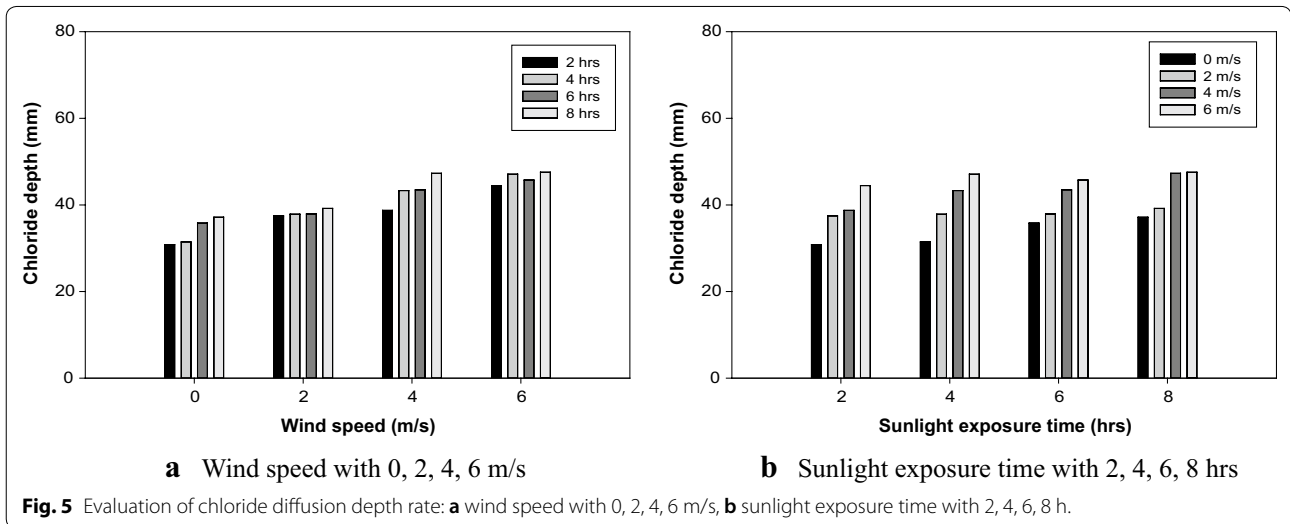
Thermo-hydrostatic curing: 23.48 (chloride diffusion coefficient rate of chamber-cured concrete at 20 °C temperature and $\pm 95\%$ relative humidity)

Wet curing: 16.78 (chloride diffusion coefficient rate of water-cured concrete at 20 °C temperature and 100% relative humidity)

Air dry curing: 43.45 (chloride diffusion coefficient rate of air-cured concrete at 20 °C temperature and $\pm 60\%$ relative humidity)

based on the colorimetric method ($\approx 0.07 \text{ N}$ for OPC), and erf^{-1} denotes the inverse error function.

Chloride diffusion coefficients rate showed a similar pattern to that of chloride penetration depths rate that is, the coefficient rate was greater at greater wind speed and sunlight exposure time. The condition with the smallest diffusion coefficient rate was the wind speed and sunlight exposure time (0 and 2) with $46.11 (\times 10^{-12} \text{ m}^2/\text{s})$. The condition with the greatest diffusion coefficient rate was the wind speed and sunlight exposure time (6 and 8) with $75.89 (\times 10^{-12} \text{ m}^2/\text{s})$, which showed about 60% difference. In addition, the diffusion coefficient rate was greater at longer sunlight exposure time, even when wind speed during curing was low, as in the case of penetration depth rate. In the comparisons between specimens of wind speed and sunlight exposure time and compared



with control specimens of water curing, thermo-hydrostatic chamber, air-drying curing, water curing with $16.78 (\times 10^{-12} \text{m}^2/\text{s})$ and wind speed and sunlight exposure time (6 and 8) with $75.89 (\times 10^{-12} \text{m}^2/\text{s})$ showed a difference of up to about 4.5 times. Regarding chloride diffusion depth rate, the maximum diffusion depth rate of the specimens cured in wind speed and sunlight exposure time (6 and 8) conditions was more than twice the minimum diffusion depth rate of the water-cured specimen.

Figures 5 and 6 show the data in Tables 5 and 6 as bar graph for comparison. As shown in Fig. 5a, the chloride diffusion depth rate results obtained from wind speed curing condition variation shows that the depth rate increases from wind speed from 0 to 6 m/s. With respect to the depth rate from sunlight exposure time curing condition variation as shown in Fig. 5b, the depth rate increases at a same rate for the wind speed variations from 0 to 4 m/s under a constant sunlight exposure time of 2, 4, 6, and 8 h.

As shown in Fig. 6a, the chloride diffusion coefficient results from wind speed curing condition variation shows that the chloride diffusion coefficient rate increases from 0 to 6 m/s. However, with respect to the chloride diffusion coefficient rate from sunlight exposure time curing condition variation shown in Fig. 6b, shows that the chloride diffusion coefficient rate increases at a same rate for the wind speed variations from 0 to 4 m/s under a constant sunlight exposure time of 2, 4, 6, and 8 h.

This is thought to occur because the considerably dried specimen of air-drying curing is highly absorbent during the experiment, and the specimens of wind speed and sunlight exposure curing have high porosity due to early water evaporation.

5 Test Results Analysis Using PBE

5.1 Satisfaction Curve of Chloride Diffusion Coefficients Rate

Figures 7, 8, 9 and 10 show Satisfaction Curves on chloride diffusion coefficients rate and chloride penetration depths rate as a function of wind speed and sunlight exposure time. Concrete durability against salt damage is evaluated by evaluating diffusion coefficients rate using Eq. (4), describes concrete specifications.

The evaluation of chloride ion diffusion coefficients rate took time-dependence into consideration, which means that diffusion coefficient rate decreases with concrete age due to change in microstructure. The durability section of the existing concrete specifications is yet to adopt this assumption in the model applied to durability evaluation. However, based on previous studies, it is thought that predicting service life of about 100 years based on diffusion coefficients rate estimated at early age of concrete can be very unreasonable and

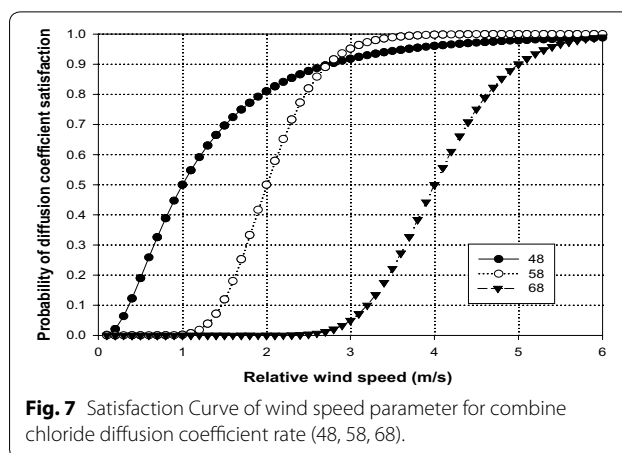


Fig. 7 Satisfaction Curve of wind speed parameter for combine chloride diffusion coefficient rate (48, 58, 68).

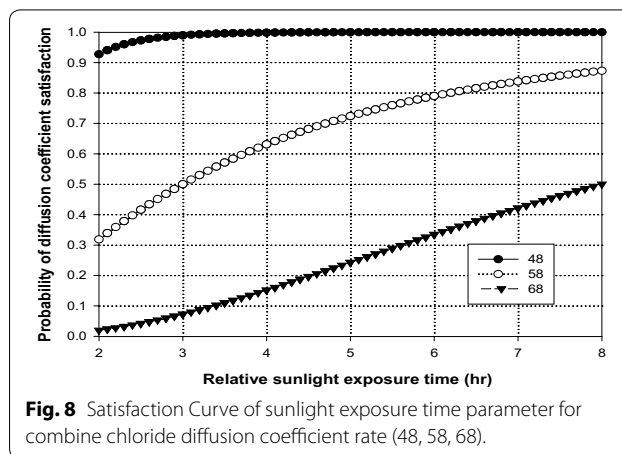


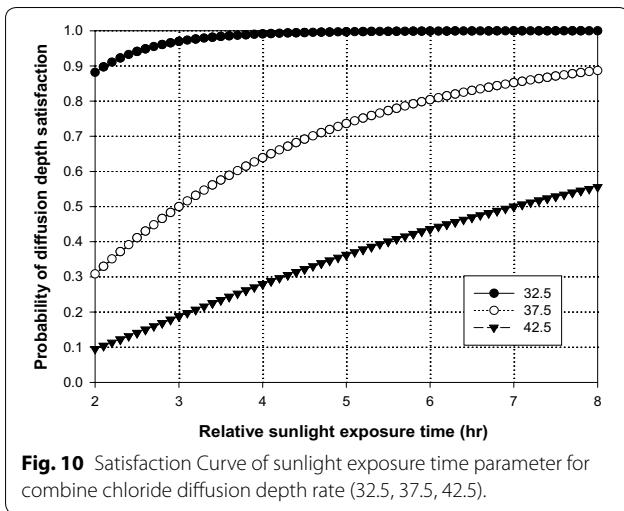
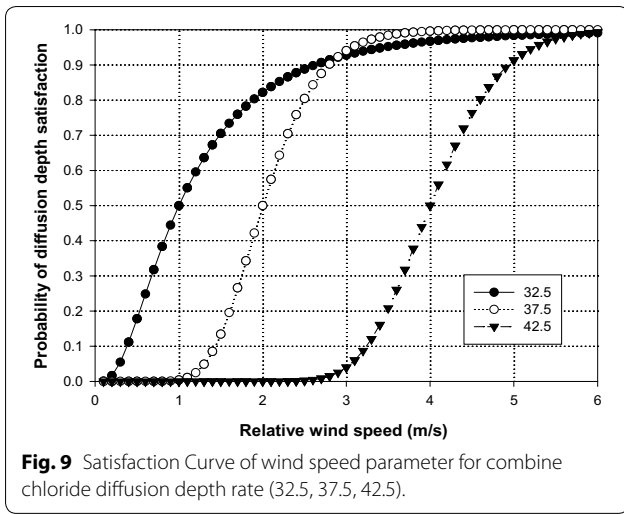
Fig. 8 Satisfaction Curve of sunlight exposure time parameter for combine chloride diffusion coefficient rate (48, 58, 68).

result in overly conservative predictions. Therefore, in the case of Eq. (4), it was adopted as a basic assumption that diffusion coefficient rate decreases over time due to hydration reaction.

$$\gamma_p D_p \leq \phi_k D_k \tag{4}$$

Here, γ_p denotes environment coefficient rate, which is generally 1.1. ϕ_k denotes durability reduction factor for salt damage, which is generally 0.86. D_k denotes the property value of concrete chloride ion diffusion coefficient rate m^2/y or m^2/y , and D_p denotes predicted value concrete chloride ion diffusion coefficient rate m^2/y or m^2/y .

In this study, with the basic assumption of decrease in diffusion coefficient rate over time, when designating $75.89 (\times 10^{-12} \text{m}^2/\text{s})$ as the wind speed and sunlight exposure (6 and 8) diffusion coefficient rate for the worst-case scenario and entering it in the Eq. (4), the predicted chloride ion diffusion coefficient rate of $58.79 (\times 10^{-12} \text{m}^2/\text{s})$ is obtained. Therefore, the required



satisfaction specification was set at $58 (\times 10^{-12} \text{m}^2/\text{s})$, and for comparative analysis of various satisfaction probabilities, diffusion coefficient rate satisfaction specifications of 48 and $68 (\times 10^{-12} \text{m}^2/\text{s})$ were added.

Figures 7, 8, 9 and 10 show the Satisfaction Curves on chloride diffusion coefficients rate, and satisfaction specifications of $(48, 58, \text{ and } 68) (\times 10^{-12} \text{m}^2/\text{s})$ were applied. Regarding evaluation of Satisfaction Curves, in Fig. 7 (as an example), when the diffusion coefficient rate as a function of wind speed was set at $58 (\times 10^{-12} \text{m}^2/\text{s})$, to satisfy 50% probability, at least 2 m/s wind speed is required, and in the case of $48 (\times 10^{-12} \text{m}^2/\text{s})$, at least 1 m/s wind speed is required. In addition, in the case of Fig. 8, when diffusion coefficient rate was set at $58 (\times 10^{-12} \text{m}^2/\text{s})$, to satisfy at least 80% satisfaction probability, 6 h of curing sunlight exposure time is required.

These demonstrate that evaluation of Satisfaction Curves based on the designer’s required criterion is possible in PBE. Given this advantage, PBE can be applied in construction sites in a wide range of environments to prevent casualties and property damages.

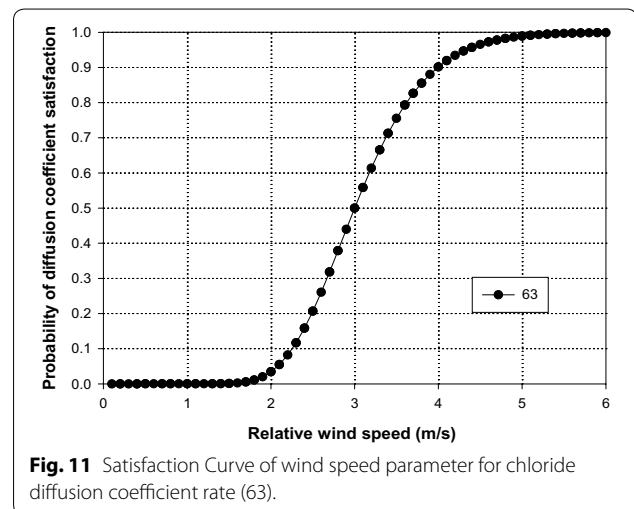
5.2 Satisfaction Curve of Chloride Diffusion Depth Rate

Figures 9 and 10 show the Satisfaction Curves on chloride penetration depth rate as a function of wind speed and sunlight exposure time, and chloride penetration depth rate can be set at (32.5, 37.5, 42.5) mm using Eq. (3). The graphs, however, show that chloride penetration depth rate (32.5, 37.5, 42.5) mm is in proportion to chloride diffusion coefficient rate (48, 58, 68) $(\times 10^{-12} \text{m}^2/\text{s})$, and Satisfaction Curves are nearly identical. In the case of Fig. 9, the 50 and 90% probabilities to satisfy designer’s required satisfaction specification, 42.5 mm requires 4 m/s and 5 m/s curing conditions. In addition, in the case of Fig. 10 of sunlight exposure time, the 20 and 50% probabilities to satisfy designer’s required satisfaction specification of 42.5 mm requires 3 h and 7 h curing conditions. In this PBE, various criteria can be set for designers’ various required targets, and the results of setting required satisfaction criteria by changing chloride ion diffusion coefficient rate to $63 (\times 10^{-12} \text{m}^2/\text{s})$ are shown in Figs. 11 and 12.

6 Code Case of Future Climate Scenario

6.1 Results of Scenario Application

In this study, it is possible to predict future climate by using various climate variables and drawing on predicted scenarios provided by KMA (Weather Knowledgebase 2012). In the past, the Special Report on Emission Scenario (SRES) based on greenhouse gas (GHG) emission, which was used in the fourth assessment report of the



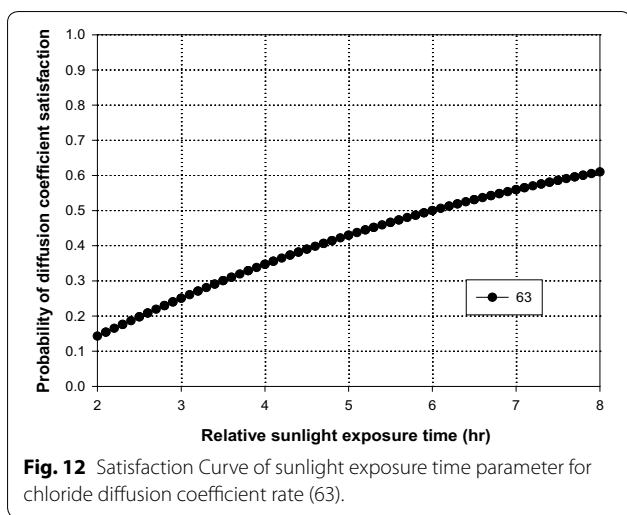


Fig. 12 Satisfaction Curve of sunlight exposure time parameter for chloride diffusion coefficient rate (63).

Intergovernmental Panel on Climate Change (IPCC), included radiative forcing regarding the impact of GHG and aerosol only among manmade climate change factors. However, more advanced Representative Concentration Pathways (RCP) scenarios are currently used. In the RCP scenarios, the term, Representative, indicates that various socioeconomic scenarios exist with regard to radiative forcing for anthropogenic GHG specified in the fifth assessment report of IPCC and the term of Pathways is used to emphasize the change over time in GHG emission scenarios. Therefore, in the present study, RCP 8.5 scenario, which assumes the highest level of GHG emission among RCP scenarios, is used to estimate various climate changes such as wind speed and sunlight exposure time in 2050, and concrete construction measures are examined accordingly.

The present study used RCP 8.5, which assumes the highest GHG emission values among the various RCP scenarios, in order to investigate the most extreme predicted climate. The application of the KMA’s program (Fig. 13) can generate various future estimates for climate factors such as temperature, relative humidity, wind speed, and precipitation, except for the sunlight exposure time, which is required in this study (Weather Knowledgebase 2012). Accordingly, the sunlight exposure time was estimated by inversely applying the results of applying the precipitation scenario, based on the logic that sunlight exposure time decreases as precipitation increases. The following conclusions were drawn from the results obtained using the procedure.

Tables 7 and 8 are the results of comparative analysis of wind speeds and sunlight exposure time at present and in future between 2046 and 2066, based on RCP 8.5

scenario. Figure 14 shows the results of applying Tables 7 and 8 to Satisfaction Curves. Regarding the low satisfaction probability of chloride diffusion coefficient rate, since its primary reason is porosity, the problem can be addressed by minimizing porosity through reduction in W/C, fine aggregate ratio, and unit water content when mixing.

6.2 Solutions to the Concrete Chloride Diffusion Coefficients Rate Problem

The following solutions based on literature are proposed to increase concrete chloride diffusion coefficients rate. Concrete chloride diffusion can degrade performance of reinforced concrete structures by causing corrosion of reinforcement bars. This problem can be resolved by increasing watertightness through increasing concrete strength, and the use of chemical and mineral admixtures. In terms of admixture, increasing slag by about 40% can reduce diffusion coefficient rate to about 40%. Coating the surface of concrete or reinforcement bars was also found to increase resistance by decreasing corrosion speed by 30-fold, while epoxy coating and nano-composite hybrid-type polymer coating decrease diffusion by 50% and 90%, respectively (Kim et al. 2009; Park et al. 2003; Lee et al. 2006). Through these various methods, concrete durability can be enhanced.

7 Conclusions

In this study, experimental evaluations were carried out to determine the effects of wind speed, and sunlight exposure time curing conditions from climate change factors on concrete strength and chloride diffusion coefficient rate. Then, Satisfaction Curves were drawn for the performance based evaluation using the Bayesian statistical method. The results obtained in the present study can be summarized as follows.

1. In the present study, the results on compressive and splitting tensile strengths according to wind speed and sunlight exposure time curing conditions suggest that 3-day and 7-day early strengths show normal development, but 28-day long-term strengths showed approximately 40% reduction in strengths as a whole. The reduction in strength is likely to be caused by inadequate hydration of the concrete specimens due to sustained wind and sunlight exposure during curing.
2. Regarding chloride diffusion depth rate and coefficients rate for concrete, compared to the condition of wind speed and sunlight exposure time (0 and 2), the

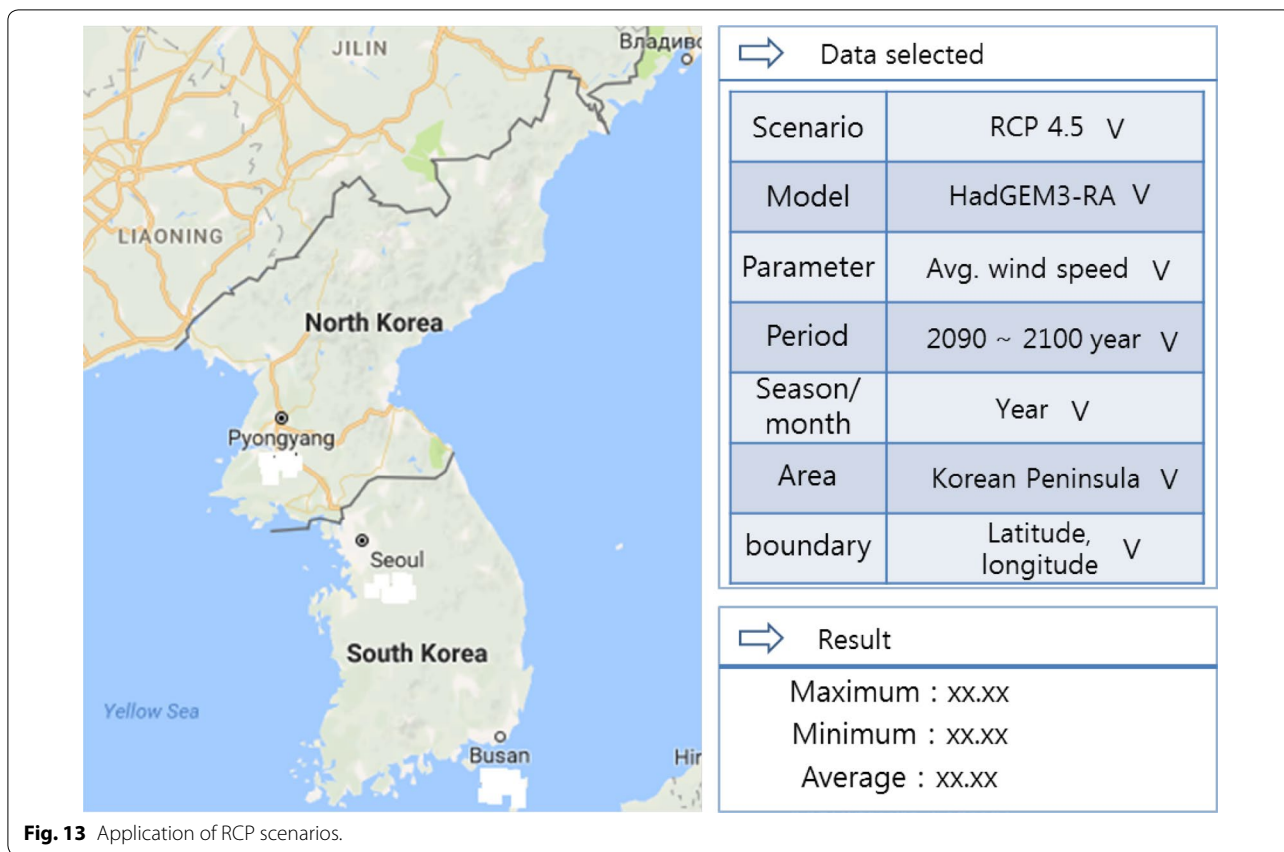


Fig. 13 Application of RCP scenarios.

Table 7 Change in wind speed by RCP scenario.

Wind speed (m/s)		
Period	Past 10 (years)	2046–2055 (years)
Jan.	2.35	2.69
Feb.	2.54	2.99
Mar.	2.83	3.3
Apr.	2.83	3.16
May	2.5	2.45
Jun.	2.36	2.24
Jul.	2.31	2.48
Aug.	2.34	2.26
Sep.	2.05	2.26
Oct.	2.05	2.38
Nov.	2.37	2.57
Dec.	2.46	2.65

condition of wind speed and sunlight exposure time (6 and 8) yielded over 1.5 times larger chloride diffusion coefficients rate, in addition to larger diffusion depth rate. The results of the comparison between water-cured control specimens and the specimens

cured in the wind speed and sunlight exposure time (6 and 8) showed that the latter had approximately 2 times more diffusion than the former. This is likely to reflect that the specimens in the experimental curing conditions develop voids inside due to early water evaporation, which results in phenomena such as microcracks, ultimately making it easy for chloride to diffuse.

- This study conducted PBE for curing conditions of climate change using general concrete mixing. The results on chloride diffusion depth rate and coefficient rate suggest that probability of success increases as wind speed and sunlight exposure time values increase. In this phenomenon, the values from experimental conditions exceed the designer’s required criteria, which indicates sharp increase in diffusion depth rate, and suggests a reduction in durability of the structure. Finally, further efforts to expand database through high intensity mixing, and more experiments on durability and usability are needed for the successful application of climate-adaptive curing methods at construction sites where various climate changes are observed.

Table 8 Change in sunlight exposure time by RCP scenario.

Sunlight exposure time (h)		
Period	Past 10 (years)	2046–2055 (years)
Jan.	5.45	3.61
Feb.	5.74	3.94
Mar.	5.81	4.52
Apr.	6.15	3.43
May	6.48	5.95
Jun.	5.59	4.09
Jul.	2.84	3.21
Aug.	4.01	5.78
Sep.	5.11	12.43
Oct.	6.50	4.06
Nov.	5.06	3.69
Dec.	5.30	2.20

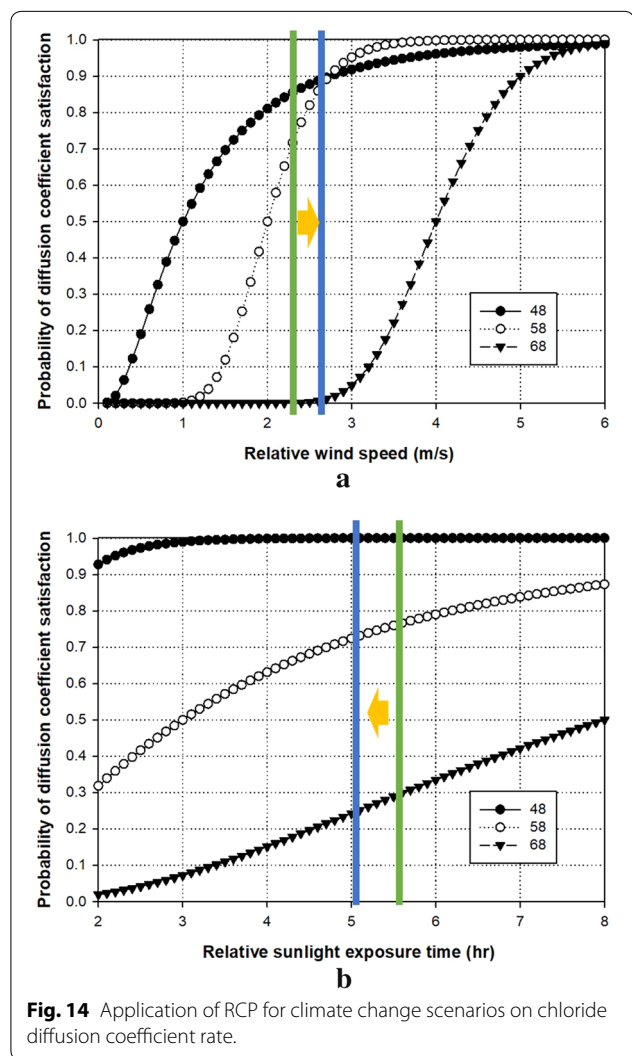


Fig. 14 Application of RCP for climate change scenarios on chloride diffusion coefficient rate.

4. As stated in the paper, this study was conducted using 100 × 200 mm cylinder specimens. However, for the application to actual construction sites, researches on larger specimens are needed. Chloride penetration damage is likely to influence concrete durability depending on the location, environment, and climatic changes. Therefore, follow-up studies need to be conducted on larger size members such as actual beams and slabs.

Authors’ contributions

TKK: A person who performed most of test and analysis works; a main writer of the paper. SJC: A person who assisted the research and writing the paper. JHC: A person who assisted the research and experiment. JHJK: A PI of the research project, who planned and developed the main idea of the study. All authors read and approved the final manuscript.

Competing interests

The authors declare that they have no competing interests.

Acknowledgements

This study was supported by the National Research Foundation of Korea (NRF) grant funded by the Korea government (MSIP) (No. 2011-0030040).

Publisher’s Note

Springer Nature remains neutral with regard to jurisdictional claims in published maps and institutional affiliations.

Received: 10 April 2017 Accepted: 29 October 2018

Published online: 01 February 2019

References

Alqam, M., & Alkam, M. K. (2014). Temperature and moisture distribution inside a circular concrete column during the early stages of hydration. *Canadian Journal of Civil Engineering*, 41(6), 556–568.

Arribas, I., Vegas, I., San-Jose, J. T., & Manso, J. M. (2014). Durability studies on steelmaking slag concretes. *Materials and Design*, 63, 168–176.

Chen, Z. T., Li, M. G., Yang, Y. Z., & Liu, Q. (2014). Restrained shrinkage behavior of concrete under different environmental conditions. *Advanced Materials Research*, 941(2), 835–841.

Dhir, R. K., & Jones, M. R. (1999). Development of chloride-resisting concrete using fly ash. *Fuel*, 78(2), 137–142.

Divsholi, B. S., Lim, T. Y. D., & Teng, S. (2014). Durability properties and micro-structure of ground granulated blast furnace slag cement concrete. *International Journal of Concrete Structures and Materials*, 8(2), 157–164.

ElSafy, A., & Abdel-Mohti, A. (2013). Investigation of likelihood of cracking in reinforced concrete bridge decks. *International Journal of Concrete Structures and Materials*, 7(1), 79–93.

Jang, S. Y., Kim, B. S., & Oh, B. H. (2011). Effect of crack width on chloride diffusion coefficients of concrete by steady-state migration tests. *Cement and Concrete Research*, 41(1), 9–19.

Kato, E., Kato, Y., & Uomoto, T. (2005). Development of simulation model of chloride ion transportation in cracked concrete. *Journal of Advanced Concrete Technology*, 3(1), 85–94.

Kim, J. H. J., Phan, D. H., Kim, B. Y., Choi, J. W., & Han, D. S. (2012). Development of satisfaction curves to evaluate concrete mix design performance using a Bayesian probabilistic method. *Construction and Building Materials*, 27(1), 578–584.

Kim, J. H. J., Phan, H. D., Yi, N. H., Kim, S. B., & Jeong, H. S. (2011). Application of the one parameter Bayesian method as the PBMD for concrete mix proportion design. *Magazine of Concrete Research*, 63(1), 31–47.

- Kim, T. K., Choi, S. J., Kim, J. H. J., & Kim, B. Y. (2015). Performance based evaluation of concrete strength under various curing conditions to investigate climate change effects. *Journal of the MDPI Sustainability*, 7(8), 10052–10077.
- Kim, T. S., Jung, S. H., Choi, Y. C., & Song, H. W. (2009). An experimental study on relation between chloride diffusivity and microstructural characteristics for GGBS concrete. *Journal of the Korea Concrete Institute*, 21(5), 639–647.
- Kim, T. K., Shin, J. H., Bae, D. H., & Kim, J. H. J. (2014). Performance based evaluation of concrete material properties from climate change effect on wind speed and sunlight exposure time curing condition. *Journal of the Korea Concrete Institute*, 26(6), 751–759.
- KMA, Korea Meteorological Administration. (2008). Understanding of climate change and climate change scenarios use. 2008
- Kwon, W. T. (2005). Current status and perspectives of climate change sciences. *Journal of Atmospheric Sciences*, 41(1), 325–336.
- Lee, D. G., Kim, M. Y., Yang, E. I., Yi, S. T., & Han, S. H. (2006). Comparison of high-durability materials for prevention of corrosion in marine concrete structures. *Proceedings Journal of the Korea Concrete Institute*, 18(2), 581–584.
- Leng, F., Feng, N., & Lu, X. (2000). An experimental study on the properties of resistance to diffusion of chloride ions of fly ash and blast furnace slag concrete. *Cement and Concrete Research*, 30(6), 989–992.
- Luping, T., & Nilsson, L. O. (1992). Rapid determination of the chloride diffusivity in concrete by applying an electrical field. *ACI Materials Journal*, 89(1), 49–53.
- Mangat, P. S., & Gurusamy, K. (1987). Chloride diffusion in steel fibre reinforced marine concrete. *Cement and Concrete Research*, 17(3), 385–396.
- Morga, M., & Marano, G. C. (2015). Chloride penetration in circular concrete columns. *International Journal of Concrete Structures and Materials*, 9(2), 173–183.
- Myong, S. J. (2009). *Current assessing vulnerability to climate change of the physical infrastructure in Korea and developing adaptation strategies* (pp. 174–182). Seoul: Korea Environment Institute.
- NT Build 492. (1999). Chloride migration coefficient from non-steady state migration experiments.
- Oh, B. H., & Jang, B. S. (2003). Chloride diffusion analysis of concrete structures considering effects of reinforcements. *ACI Materials Journal*, 100(2), 143–149.
- Park, H. W., Song, H. W., Back, J. M., Woo, J. T., & Nam, J. W. (2003). An experimental study on durability evaluation of nano composite hybrid polymer type coatings applied concrete. *Proceedings Journal of the Korea Concrete Institute*, 15(1), 687–692.
- Park, S. J., & Choi, Y. (2012). Influence of curing-form material on the chloride penetration of off-shore concrete. *International Journal of Concrete Structures and Materials*, 6(4), 251–256.
- Phan, H. D., Kim, J. H. J., Yi, N. H., You, Y. J., & Kim, J. W. (2012). Strength targeted PBMD of HSC based on one-parameter Bayesian probabilistic method. *Advanced Concrete Technology*, 10(4), 137–150.
- Poon, C. S., Kou, S. C., & Lam, L. (2006). Compressive strength, chloride diffusivity and pore structure of high performance metakaolin and silica fume concrete. *Construction and Building Materials*, 20(10), 858–865.
- Ramseyer, C., & Kang, T. H. K. (2012). Post-damage repair of prestressed concrete girders. *International Journal of Concrete Structures and Materials*, 6(3), 199–207.
- Tang, L., & Nilsson, L. O. (1992). Rapid determination of chloride diffusivity of concrete by applying an electric field. *ACI Materials*, 89(1), 49–53.
- Thomas, M. D., & Bamforth, P. B. (1999). Modelling chloride diffusion in concrete: effect of fly ash and slag. *Cement and Concrete Research*, 29(4), 487–495.
- Weather Knowledgebase (2012) KOREA Seoul, dongjak-gu. <http://www.kma.go.kr/>. Accessed 2 Mar 2012.
- Ye, H., Fu, C., Jin, N., & Jin, X. (2015). Influence of flexural loading on chloride ingress in concrete subjected to cyclic drying-wetting condition. *Computers & Concrete*, 15(2), 183–198.

Submit your manuscript to a SpringerOpen[®] journal and benefit from:

- Convenient online submission
- Rigorous peer review
- Open access: articles freely available online
- High visibility within the field
- Retaining the copyright to your article

Submit your next manuscript at ► springeropen.com
